

Prototype dispenser photocathode: Demonstration and comparison to theory

N. A. Moody, K. L. Jensen, D. W. Feldman, P. G. O'Shea, and E. J. Montgomery

Citation: [Applied Physics Letters](#) **90**, 114108 (2007); doi: 10.1063/1.2713341

View online: <http://dx.doi.org/10.1063/1.2713341>

View Table of Contents: <http://scitation.aip.org/content/aip/journal/apl/90/11?ver=pdfcov>

Published by the [AIP Publishing](#)

Articles you may be interested in

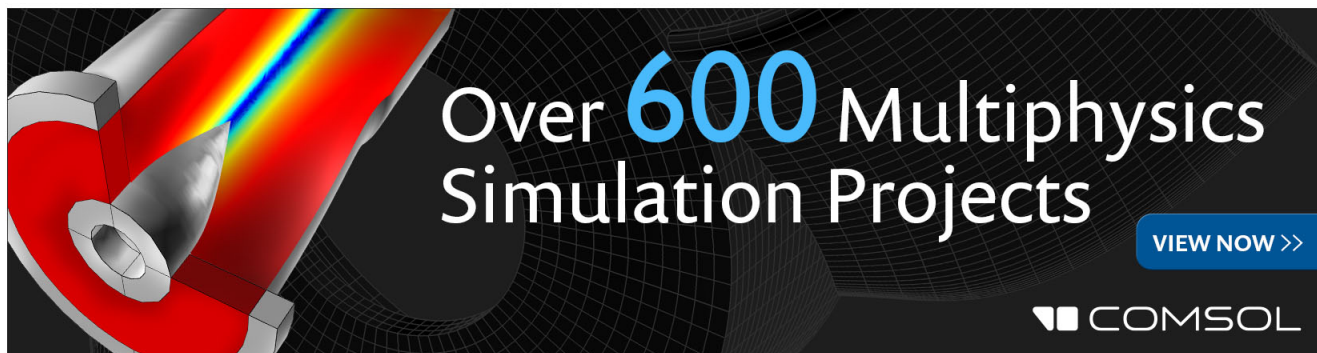
[Modeling the evaporation rate of cesium off tungsten based controlled porosity dispenser photocathodes](#)
AIP Advances **3**, 042105 (2013); 10.1063/1.4800700

[Evaluation of a cesium iodide photocathode assisted with MgO-coated multiwall carbon nanotubes](#)
Appl. Phys. Lett. **96**, 141109 (2010); 10.1063/1.3383220

[Factors affecting performance of dispenser photocathodes](#)
J. Appl. Phys. **102**, 104901 (2007); 10.1063/1.2805653

[The quantum efficiency of dispenser photocathodes: Comparison of theory to experiment](#)
Appl. Phys. Lett. **85**, 5448 (2004); 10.1063/1.1827936

[Electron diffusion length and escape probabilities for cesiated and hydrogenated polycrystalline diamond photocathodes](#)
Appl. Phys. Lett. **75**, 3533 (1999); 10.1063/1.125379

The advertisement features a 3D cutaway simulation of a cylindrical component with a red interior and a grey exterior. A blue and yellow beam of light or energy is shown entering the component. The background is dark with a grid pattern. The text 'Over 600 Multiphysics Simulation Projects' is prominently displayed in white and blue. A blue button with white text says 'VIEW NOW >>'. The COMSOL logo is in the bottom right corner.

Over **600** Multiphysics
Simulation Projects

[VIEW NOW >>](#)

COMSOL

Prototype dispenser photocathode: Demonstration and comparison to theory

N. A. Moody^{a)}

Los Alamos National Laboratory, Los Alamos, New Mexico 87545

K. L. Jensen

Naval Research Laboratory, Washington, DC 20375-5347

D. W. Feldman, P. G. O'Shea, and E. J. Montgomery

University of Maryland, College Park, Maryland 20742-3511

(Received 10 January 2007; accepted 8 February 2007; published online 15 March 2007)

A method to significantly extend the operational lifetime of alkali-based photocathodes by diffusing cesium to the surface at moderate temperature is presented and shown to restore the quantum efficiency (QE) of cesiated tungsten. Experimental measurements of QE as a function of surface cesium coverage compare exceptionally well with a recent theoretical photoemission model, notably without the use of adjustable parameters. A prototype cesium dispenser cell is demonstrated and validates the concept upon which long-life dispenser photocathodes can be based. © 2007 American Institute of Physics. [DOI: 10.1063/1.2713341]

Photoinjection produces high quality electron beams for free electron lasers (FEL's), energy-recovery linacs, pump-probe experiments, and other applications.¹ A pulsed drive laser impinges a cathode and acts to photoswitch the electron beam in synchronicity with an accelerating rf field. Many photocathode types have been intensely studied, but no single technology exhibits both high quantum efficiency (QE) and extended operational lifetime without complicated surface conditioning. A related problem is the lack of a good photoemission model for coated surfaces, needed not only for cathode development but also for end-to-end beam simulation to ascertain the impact of (for example) intrinsic photocathode emittance as it relates to emission nonuniformity and evolution. QE is not the only metric of photocathode performance: operation under laboratory conditions cannot be extrapolated to the environment of a rf gun by fiat. Here, a dispenser cathode capable of establishing and maintaining a photosensitive cesium layer on the surface via diffusion through porous sintered tungsten is demonstrated and characterized. Measurements of the QE of a partially covered surface correlated exceptionally well with a theoretical model, notably without the use of adjustable parameters. Based on the temperature-related behavior of the prototype, it is argued that a controlled porosity dispenser photocathode (CPDP) is a viable electron source candidate for high power FEL's.

Metallic emitters, though extremely robust, require a UV drive laser and exhibit very low QE. Multialkali photocathodes (e.g., CsK₂Sb and Cs₃Sb) have impressive QE in the visible range but degrade quickly even in ultrahigh vacuum,² believed to be because loss of one or more alkali components occurs from the cathode surface due to chemical instability. A remedy in the case of cesium-based photocathodes is re-coating the surface with trace amounts of cesium to restore optimal photosensitivity.³ For most photoinjector designs, replacement of surface monolayers requires complex procedures at regular intervals. The advantage of the CPDP archi-

ture is the possibility of *in situ* monolayer replenishment of cesium that may, in turn, extend the lifetime of high QE alkali-based photocathodes.

Dispenser cathodes are a mature thermionic emitter technology.⁴⁻⁶ The work function is lowered as the alkali material trapped in a porous tungsten matrix diffuses to the surface at high temperature. Traditional dispenser thermionic cathodes operate much hotter (>1000 °C) than the breakdown temperature of high QE films (~220 °C). We advocate instead a prototype dispenser cell which operates at 180 °C using sintered tungsten as a diffusion barrier encapsulating a sealed volume of cesium chromate. Initial activation at 500 °C releases elemental cesium within the cell, and subsequent heating to 180 °C allows its controlled diffusion to the cathode surface. The lower operating temperature significantly reduces evaporative losses and accommodates deposition growth of highly photosensitive surface layers following the initial activation heating.

The effect of cesium on the substrate material (tungsten) was studied in detail,^{7,8} by measuring QE while cesium was evaporated onto the substrate surface using external, commercial alkali sources. The amount of cesium arriving at the surface was measured using a quartz crystal balance. In the dispenser cell, cesium arrives from beneath the substrate, so surface coverage cannot be directly measured as before but can be theoretically inferred based on the established relationship between QE and cesium coverage,⁹ which therefore provides a method to measure the amount of cesium at the cathode surface. Using this technique, it was confirmed that after activation the dispenser cell released cesium to the surface at a controlled rate at temperatures less than 200 °C. Importantly, QE measurements suggest that the layer uniformly coats the surface as in the case where cesium is evaporated directly onto a solid tungsten metal base.

The sintered tungsten dispenser substrate is roughly 30% porous and was cleaned prior to deposition using a 40 mA dose of a 6.4 keV argon ion beam. Photocurrent was measured using diode lasers (<5 mW) at five different wavelengths (375, 405, 532, 655, and 802 nm). Further details of

^{a)}Electronic mail: nmoody@ieee.org

the experimental apparatus are deferred to a later work. The relationship between QE and cesium coverage is highly repeatable when an argon ion beam cleaning is performed at least once prior to each deposition and agreement with the updated theoretical model (below) is excellent. After the initial argon ion dose, additional cleaning did not produce higher QE. The base pressure of the UHV system was maintained at 3×10^{-10} Torr, reaching 2×10^{-9} Torr during the cesium deposition process because of the slight outgassing of the source.

Agreement between theory and experiment was markedly improved based on two modifications to the previous model:⁹ a revised model of the temperature and energy dependent electron scattering terms and the use of an updated moment-based approach¹⁰ to emission probability. The scattering terms considered are electron-acoustic phonon and electron-electron (for which the latter dominates in metals) coupled with a low-temperature residual scattering rate. The electron-phonon relaxation rate is modeled by^{11,12}

$$\tau_{ac} = \frac{\pi \rho \hbar^3 v_s^2}{m k_B T k_F \Xi^2} \left(\frac{T_D}{T} \right)^5 \left\{ \int_0^{T_D/T} \frac{x^5 dx}{(e^x - 1)(1 - e^{-x})} \right\}^{-1}, \quad (1)$$

where v_s is the velocity of sound, Ξ is the deformation potential, $\hbar k_F$ is the Fermi momentum, and T_D is the Debye temperature. The electron-electron relaxation time^{13,14} is modeled by

$$\tau_{ee} = \frac{8 \hbar K_s^2}{\alpha^2 \pi m c^2 (k_B T)^2} \left[\left(1 + \left(\frac{\Delta E}{\pi k_B T} \right)^2 \right) \gamma \left(\frac{2 k_F}{q_o} \right) \right]^{-1},$$

$$\gamma(x) = \frac{x^3}{4} \left(\tan^{-1} x + \frac{x}{1+x^2} - \frac{\tan^{-1}(x\sqrt{2+x^2})}{\sqrt{2+x^2}} \right), \quad (2)$$

where K_s is a dielectric constant modification which accounts for additional screening by d electrons, α is the fine structure constant, ΔE is the electron energy above the Fermi level, $\hbar k_F$ is the Fermi momentum, and q_o is the Thomas-Fermi screening factor. By using a combination of commonly available temperature-dependent thermal conductivity data and Monte Carlo simulations of electron-electron scattering rates as a function of energy from the literature only, we have inferred appropriate values of Ξ and K_s and the low temperature residual scattering rate. Using these values without modification, we have compared the theoretical model to QE measurements from tungsten and silver surfaces partially coated with cesium. The details of the parameter determination and qualification for the scattering terms based on values in the literature and the methods for solving the moment-based integrals in the presence of a work function which depends on surface coverage of cesium will be deferred to a separate publication.

Figures 1 and 2 compare experimental data to theoretical predictions. The relationship between the experimental coordinate (thickness of cesium deposited on the surface) and the theoretical coordinate (percentage of surface covered) is related by the cesium covalent radius of 0.52 nm: the mass of a monolayer corresponds to the density of cesium multiplied by the area coated and the thickness of the monolayer. All theoretical values used in the calculation were independently obtained based on literature sources and not adjusted to optimize agreement with experiment. The theory/experiment agreement, both in the relative dependence highlighted on

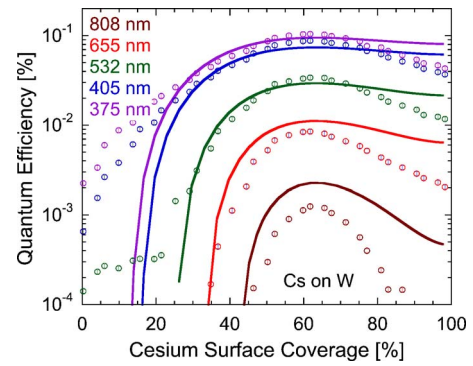


FIG. 1. (Color online) Theoretical and experimental agreement (relative) for QE vs cesium coverage.

the log scale and in an absolute sense, for cesium on tungsten following an argon ion cleaning, is extraordinarily good. Discrepancies arise for the lower photon energies that may be related to nonuniform coverage effects and other factors that will be explored in greater detail elsewhere. To test whether the agreement was fortuitous, the same experiment was performed for cesium deposited on a silver surface. The level of agreement was again good (see Fig. 4 in Ref. 15), suggesting that the theoretical model adequately accounts for the physics involved and provides a sufficiently qualified emission model for complex beam simulation codes.¹⁶ For all wavelengths and both base metal cases, theory and experiment agree quite well, an encouraging observation given the complexity of the polycrystalline photoemitting surface, especially when microscopic features such as grain crystal face, contaminants, and pores are evident, which the theory at present treats as uniform. Since work function can vary several tenths of an electron volt depending on crystal orientation, micron-scale resolution in a photoemission electron microscope system¹⁷ as well as temperature variation effect studies may be required in order to discern systematic variation between theory and experiment. These experiments are in preparation.

The relationship between QE and cesium coverage on (atomically clean) sintered tungsten can be used to infer the arrival of cesium to the surface of the dispenser cell by monitoring QE. The dispenser cell consists of a thin-walled stainless steel canister 1 cm in height and diameter with a 1 mm thick sintered tungsten disk brazed to the top. Powders of cesium chromate and titanium (1:5 weight ratio) were pressed into a 0.7 gm pellet and inserted into the cell prior to brazing. The cell was then evacuated and outgassed at

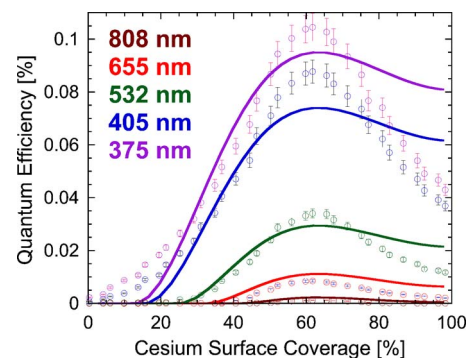


FIG. 2. (Color online) Theoretical and experimental agreement (absolute) for QE vs cesium coverage.

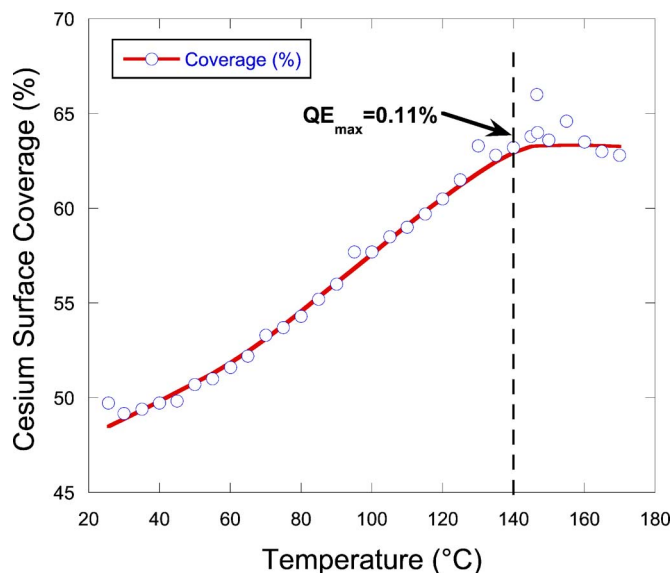


FIG. 3. (Color online) Cesium coverage vs temperature during dispenser cathode rejuvenation.

225 °C. Activation occurred upon further heating to 470 °C when cesium chromate reacted with titanium powder, releasing elemental cesium. Most of the elemental cesium was contained within the cell, but some escaped and accumulated on chamber walls and contributed to thermionic emission from the cathode surface. The cell was cooled to room temperature, allowing cesium to remain within the cell and to accumulate on its surface. QE was measured continuously for several days until the cesium layer began to degrade, resulting in a decreased photoyield from 0.11% to 0.06% in the UV (375 nm). Upon heating from room temperature, QE increased as cesium was brought to the surface to repair the damaged layer, and at 140 °C, QE reached its previous peak value of 0.11% in the UV. Argon ion cleaning was used to remove the entire surface layer and return to an atomically clean tungsten substrate. The dispenser was again slowly heated to bring cesium to the surface, and the previous increase and peak in QE was again observed. These results demonstrate that the dispenser cell can deliver cesium to the surface in a controlled manner at moderate temperatures (≤ 150 °C).

Relating QE to cesium coverage quantifies the ability of the dispenser to deliver cesium to the surface. Figure 3 shows coverage as a function of temperature during the rejuvenation cycle. Note that at 140 °C (the temperature at which QE peaks) the coverage is observed to be about 63%. Coverage does not increase beyond this value because the elevated temperature causes desorption which prevents further accumulation of cesium at the surface. The $1/e$ lifetime for a re-cesiated layer at room temperature was about 5 days. QE decreases over time because cesium leaves the surface either through desorption or because of ion back-bombardment. If the cell is held at an elevated temperature, however, the cesium layer can be continuously repaired. An

initial cesium layer was placed on the dispenser cell and then heated to 180 °C continuously while QE was measured for more than 8 days. The $1/e$ lifetime of the cathode during this continuous rejuvenation process was increased by roughly an order of magnitude to more than 47 days. This confirms that the rejuvenation process can be sustained over extended periods.

In conclusion, the QE of a Cs-covered sintered tungsten surface was characterized, and the data were shown to correlate well with a photoemission model. Experiment and theory agree to within 30%, and the relationship between QE and cesium surface coverage was used to investigate and characterize a prototype dispenser photocathode. The dispenser surface was cleaned using an argon ion beam and activated at 470 °C. Subsequent heating at much lower temperatures (140–180 °C) allowed a controlled release of cesium to the surface that established and maintained a surface layer optimal for photoemission. The dispenser cell was shown to deliver cesium to the surface in a temperature controlled manner over long periods of time. The determination of whether high QE cathodes can be built based on the dispenser cell technology and rejuvenated *in situ* to provide uniform surface coverage and good QE at operational temperatures will be the subject of a separate work.

The authors gratefully acknowledge funding provided by the Joint Technology Office and the Office of Naval Research. The authors have benefited from interactions with David Dowell (SLAC), Jonathan Shaw (NRL), Joan Yater (NRL), Dinh Nguyen (LANL), and John Smedley (BNL).

- ¹P. G. O'Shea and H. P. Freund, *Science* **292**, 1853 (2001).
- ²S. H. Kong, *Nucl. Instrum. Methods Phys. Res. A* **358**, 272 (1995).
- ³A. H. Sommer, *Photoemissive Materials*, 1st ed. (Wiley, New York, 1968), Chap. 8, pp. 113–199.
- ⁴W. C. Rutledge and E. S. Rittner, *J. Appl. Phys.* **28**, 167 (1957).
- ⁵G. Gärtner, P. Geittner, D. Raasch, and D. U. Wiechert, *Appl. Surf. Sci.* **146**, 22 (1999).
- ⁶R. T. Longo, *J. Appl. Phys.* **94**, 6966 (2003).
- ⁷N. A. Moody, D. W. Feldman, and P. G. O'Shea, *J. Directed Energy* (to be published).
- ⁸N. A. Moody, D. W. Feldman, P. G. O'Shea, K. L. Jensen, and A. Balter, *Proceedings of the 27th International Free Electron Laser Conference, Stanford, CA (2005)*, p. MOPP050, www.bessy.de/fel2006/
- ⁹K. L. Jensen, D. W. Feldman, N. A. Moody, and P. G. O'Shea, *J. Appl. Phys.* **99**, 124905 (2006).
- ¹⁰K. L. Jensen, P. G. O'Shea, D. W. Feldman, and N. A. Moody, *Appl. Phys. Lett.* **89**, 224103 (2006).
- ¹¹B. K. Ridley, *Quantum Processes in Semiconductors*, 4th ed. (Clarendon, Oxford, 1999).
- ¹²Harald Ibach, and Hans Lüth, *Solid State Physics*, 2nd Ed. (Springer, Berlin, 1995).
- ¹³D. K. Wagner and R. Bowers, *Adv. Phys.* **27**, 651 (1978).
- ¹⁴A. V. Lugovskoy and I. Bray, *J. Phys. D* **31**, L78 (1998).
- ¹⁵K. L. Jensen, N. A. Moody, D. W. Feldman, P. G. O'Shea, J. E. Yater, and J. L. Shaw, *Proceedings of the 28th International Free Electron Laser Conference, Berlin, Germany, 2006* (unpublished), Paper No. THPPH068.
- ¹⁶J. J. Petillo, presented at 48th Annual Meeting of the Division of Plasma Physics (APS), Philadelphia, PA, 2006 (unpublished).
- ¹⁷J. Shaw, J. Yater, K. L. Jensen, P. G. O'Shea, D. W. Feldman, and N. A. Moody, presented at Ninth Annual Directed Energy Symposium, Albuquerque, NM, 2006 (unpublished).